J|A|C|S COMMUNICATIONS

Published on Web 04/25/2006

Periodic Mesoporous Organosilica Hollow Spheres with Tunable Wall Thickness

H. Djojoputro,[†] X. F. Zhou,[‡] S. Z. Qiao,[†] L. Z. Wang,[†] C. Z. Yu,[†,‡] and G. Q. Lu*,[†]

ARC Centre for Functional Nanomaterials, School of Engineering, The University of Queensland, St. Lucia, QLD 4072, Australia, and Department of Chemistry, Shanghai Key Laboratory of Molecular Catalysis and Innovative Materials, Fudan University, Shanghai 200433, P.R. China

Received February 13, 2006; E-mail: maxlu@uq.edu.au

Since their first report in 1992,[1] self-assembled mesoporous silicates and aluminosilicates have attracted much attention in material science.[2,3] In addition to the success in nonsiliceous mesoporous materials,[4] a significant breakthrough in this field was the discovery of periodic mesoporous organosilica (PMO), which contains organic groups homogeneously distributed in the silica framework.[5,6] Compared to mesoporous silica, it is easier to tailor the chemical and physical properties of PMO by adjusting the organic bridging groups, which leads to potential applications in microelectronics, protein separation, catalysis, and biosensing.[7]

It is useful to design the morphology of mesoporous material in order to facilitate the desired application. Mesoporous hollow spheres are very attractive due to their outstanding properties of low density, high surface area, and well-defined mesoporous wall structures that bring high permeability for controlled mass transport; hence, they can be used as confined nanocatalysts, adsorbents, targeted drug and gene delivery, as well as biomolecule encapsulation. The synthesis strategy generally involves the sonochemical method,[8] the fluorinated surfactant templating,[9] and the emulsion templating.[10,11] However, only few examples of hollow spheres with ordered mesoporous wall structure were reported.[12] Furthermore, there is no good control over the wall thickness of hollow spheres in previous reports. In addition, to the best of our knowledge, there has been no report of hollow spheres with PMO wall compositions.

Here we report a successful synthesis of PMO hollow spheres with tunable wall thickness by a new vesicle and a liquid crystal "dual templating" approach (Scheme 1). Fluorocarbon surfactant $[C_3F_7O(CFCF_3CF_2O)_2CFCF_3CONH(CH_2)_3N^+(C_2H_5)_2CH_3I^-]$ (FC4) and cationic surfactant cetyltrimethylammonium bromide (CTAB) were employed as costructure directing agents and 1,2-bis(trimethoxysilyl)ethane (BTME) as the hybrid silica precursor. FC4 and organosilica may self-assemble into vesicles through a vesicle templating (VT) process; meanwhile, organosilica and CTAB composite micelles further pack surrounding the vesicles as "nucleation" sites by a liquid crystal templating (LCT) process which determines the final wall structure. Importantly, the PMO hollow spheres possess highly ordered hexagonal mesostructured walls, and the wall thickness can be adjusted in a certain range.

In a typical synthesis of PMO hollow spheres, 0.3 g of FC4 was dissolved in 96 g of water and stirred at room temperature for 1 h before the addition of 0.2 g of CTAB and 0.7 mL of 2 M NaOH. Then the system is kept at constant temperature of 80 °C, and 0.655 mL of BTME was introduced under vigorous stirring. The reactant molar ratio of FC4:CTAB:BTME:H_2O:NaOH is 0.6:1:4.7:9700:2.5. After 2 h, the white precipitates were collected by filtration and dried at room temperature. To remove the surfactant, the above as-synthesized samples were refluxed in the mixture of ethanol and HCl for 24 h at 50 °C. To understand the formation mechanism of PMO hollow spheres, the FC4/CTAB molar ratio (X) was varied (0, 0.2, 0.6, 1.2) while keeping the other reaction conditions constant.

Scheme 1. Schematic Representation of the Vesicle Templating (VT) and the Liquid Crystal Templating (LCT) Dual Templating Process

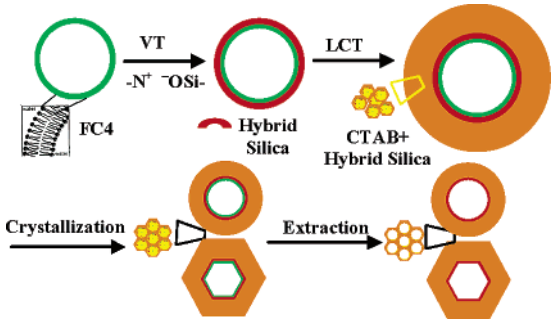

Powder X-ray diffraction (XRD) patterns of PMO samples synthesized at different X are shown in Figure 1. In the absence of FC4 ($X = 0$), the surfactant-extracted sample exhibits a highly ordered cubic mesostructure (symmetry: *Pm*3*n*). The transmission electron microscopy (TEM) image recorded along the [100] direction shows the typical cubic pattern of a *Pm*3*n* symmetry (Figure 2a),[13] in accordance with the XRD results. The scanning electron microscopy (SEM) observations reveal a solid spherical morphology. The diameters of particles are in the range of 500−1000 nm (Figure S1a).

For the sample synthesized at $X = 0.2$ (Figure 1b), the mesostructure is obviously different from that obtained without FC4, which can be attributed to the transition state from a cubic *Pm*3*n* to a 2D hexagonal *p*6*m* structural transformation (see below). SEM images reveal a spherical morphology with diameters in the range of 300−800 nm (Figure S1b). TEM image shows that the hollow parts exist in some spheres (Figure 2b), although the dimension of the cavity is relatively small compared to the volume of one sphere.

When $X = 0.6$, the XRD pattern reveals a highly ordered 2D hexagonal structure (Figure 1c). From SEM observations, the diameters of particles are in the range of 300−500 nm (Figure S1c). A certain degree of agglomeration between particles is observed. Some broken particles suggest that these materials are indeed hollow. TEM images show hollow particles with either spherical or hexagonal shapes (Figure 2c), and the highly ordered hexagonally arrayed wall mesostructure is very clear at a higher magnification (Figure 2d). The size of the hollow part is about 100−150 nm, with the wall thickness around 100 nm. Some cavities are also in hexagonal shape, which is unusual compared to other mesoporous hollow spheres where generally spherical cavities are observed. Another interesting feature of PMO hollow spheres synthesized by

[†] The University of Queensland.
[‡] Fudan University.

10.1021/ja0607537 CCC: $33.50

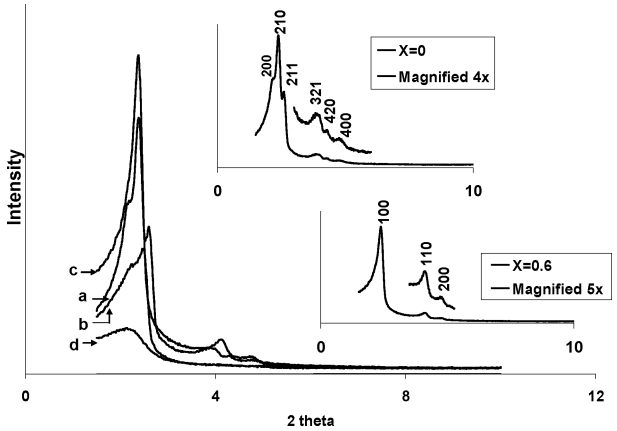

Figure 1. XRD patterns (a), (b), (c), and (d) of surfactant-removed samples synthesized at FC4/CTAB molar ratio $X = 0$, 0.2, 0.6, and 1.2, respectively.

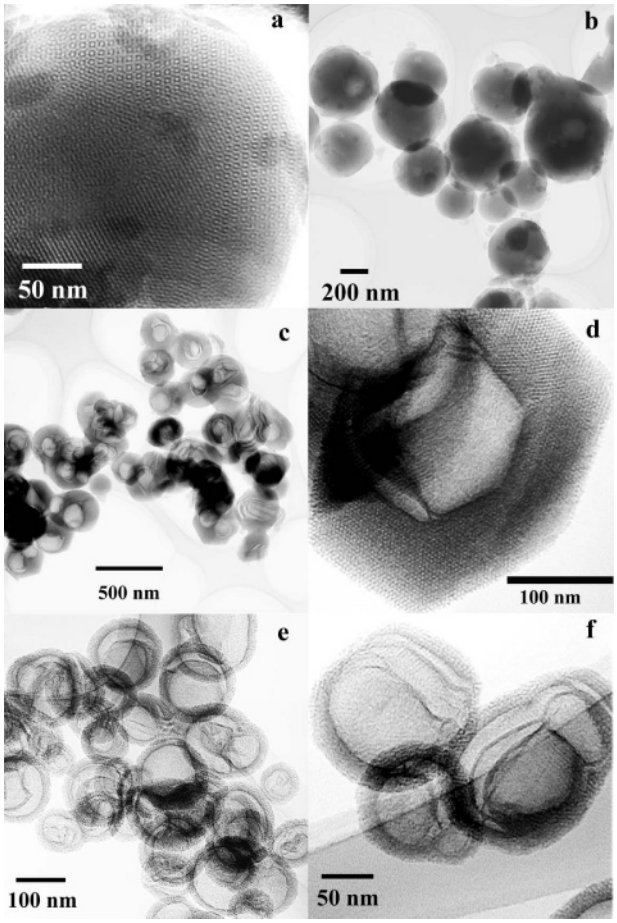

Figure 2. TEM images (a), (b), (c, d), and (e, f) of surfactant-removed PMO materials synthesized with FC4/CTAB molar ratio $X = 0$, 0.2, 0.6, and 1.2, respectively.

FC4 and CTAB co-templates is the abnormal "shell" structure inside the cavities. It is quite clear that a thin spherical shell exists within the cavities (Figure 2c and 2d).

Further increasing the FC4/CTAB molar ratio to $X = 1.2$ leads to a broad XRD peak (Figure 1d) with decreased particle size (~200 nm, Figure S1d). TEM observations (Figure 2e,f) reveal that the cavity size is ~50−100 nm, while the wall thickness is ~20 nm. The mesostructure is less ordered than those synthesized at $X = 0.6$. The shell structure inside the cavity can also be observed. For comparison, the physicochemical properties of PMO samples synthesized at different X are summarized in Table S1.

We propose that, when FC4 and CTAB are used as co-templates in our synthesis, the cationic FC4 may interact with the negatively charged silica species to generate composite vesicles through a vesicle templating process (Scheme 1, see also Figure S3).[14] Subsequently, these vesicles act as a "nucleus" for further growth of micelle-templated mesoporous materials surrounding them, where a liquid crystal templating process may determine the final wall structure. It is supposed that the composite vesicles are quite flexible in solution; hence, the mesostructure of surrounding walls may influence the shape of particles and cavities. When the wall has a hexagonal mesostructure at $X = 0.60$, some particles as well as their cavities may follow a hexagonal shape to correspond to their mesostructure. On the removal of templates, it will generate PMO hollow spheres with mesoporous walls, and the nucleus vesicle is left as a shell inside the cavities.

The above dual templating mechanism can also explain the wall thickness and mesostructure changes of PMO materials synthesized at different amounts of FC4 and the same temperature of 80 °C. With increase in X, the number of nuclei formed by FC4 and hybrid silica source increases; hence, the hybrid silica available to pack around each nucleus decreases, leading to reduced wall thickness and size of hollow particles. Moreover, by increasing X, the amount of hybrid silica available to interact with CTAB decreases. The decreased curvature[15] of a composite hybrid silica/CTAB micelle leads to the transformation from *Pm*3*n* to *p*6*m* mesostructure.

In conclusion, the PMO hollow spheres with highly ordered mesoporous wall structure, tunable particle size, and wall thickness are successfully synthesized by this novel vesicle and liquid crystal dual templating approach. This method might be applicable to produce hollow spheres with other compositions for versatile applications in drug and DNA delivery, biomolecular encapsulation, or as nanoreactors for biological reactions at the molecular levels.

Acknowledgment. This work was partially supported by the Australian Research Council (ARC) of discovery program (DP0452461) and the ARC Centre for Functional Nanomaterials.

Supporting Information Available: SEM images, N_2 sorption isotherms, and physicochemical properties of samples synthesized at different X. TEM images of PMO samples templated by FC4. This material is available free of charge via the Internet at http://pubs.acs.org.

References

(1) Kresge, C. T.; Leonowicz, M. E.; Roth, W. J.; Vartuli, J. C.; Beck, J. S. *Nature* **1992**, *359* (6397), 710−712.
(2) Stein, A. *Adv. Mater.* **2003**, *15* (10), 763−775.
(3) Davis, M. E. *Nature* **2002**, *417* (6891), 813−821.
(4) Yu, C. Z.; Tian, B. Z.; Zhao, D. Y. *Curr. Opin. Solid State Mater. Sci.* **2003**, *7* (3), 191−197.
(5) Inagaki, S.; Guan, S.; Fukushima, Y.; Ohsuna, T.; Terasaki, O. *J. Am. Chem. Soc.* **1999**, *121* (41), 9611−9614.
(6) Asefa, T.; MacLachan, M. J.; Coombs, N.; Ozin, G. A. *Nature* **1999**, *402* (6764), 867−871.
(7) Hatton, B.; Landskron, K.; Whitnall, W.; Perovic, D.; Ozin, G. A. *Acc. Chem. Res.* **2005**, *38* (4), 305−312.
(8) Rana, R. K.; Mastai, Y.; Gedanken, A. *Adv. Mater.* **2002**, *14* (19), 1414−1418.
(9) Tan, B.; Lehmler, H. J.; Vyas, S. M.; Knutson, B. L.; Rankin, S. E. *Adv. Mater.* **2005**, *17* (19), 2368−2371.
(10) Sun, Q. Y.; Kooyman, P. J.; Grossmann, J. G.; Bomans, P. H. H.; Frederik, P. M.; Magusin, P.; Beelen, T. P. M.; van Santen, R. A.; Sommerdijk, N. *Adv. Mater.* **2003**, *15* (13), 1097−1100.
(11) Yu, C. Z.; Tian, B. H.; Fan, J.; Stucky, G. D.; Zhao, D. Y. *Chem. Lett.* **2002** (1), 62−63.
(12) Li, Y. S.; Shi, J. L.; Hua, Z. L.; Chen, H. R.; Ruan, M. L.; Yan, D. S. *Nano Lett.* **2003**, *3* (5), 609−612.
(13) Sakamoto, Y.; Kaneda, M.; Terasaki, O.; Zhao, D. Y.; Kim, J. M.; Stucky, G.; Shim, H. J.; Ryoo, R. *Nature* **2000**, *408* (6811), 449−453.
(14) Hubert, D. H. W.; Jung, M.; Frederik, P. M.; Bomans, P. H. H.; Meuldijk, J.; German, A. L. *Adv. Mater.* **2000**, *12* (17), 1286−1290.
(15) Huo, Q.; Margolese, D. I.; Stucky, G. D. *Chem. Mater.* **1996**, *8* (5), 1147−1160.

JA0607537